Journal of Applied Polymer Science

Effect of the Preparation Conditions on the Morphology and Performance of Poly(imide) Hollow Fiber Membranes

Qusay F. Alsalhy,[1] Haydar A. Salih,[1] Remonda H. Melkon,[2] Yusra M. Mahdi,[2] Noora A. Abdul Karim[2]

[1]Membrane Technology Research Unit, Chemical Engineering Department, University of Technology, Alsinaa Street 52, Baghdad, Iraq

[2]Chemical and Petrochemical Research Center, Corporation of Research and Industrial Development, Ministry of Industry & Minerals, Baghdad, Iraq

Correspondence to: Q. F. Alsalhy (E-mail: qusay_alsalhy@yahoo.com; qusayalsalhy@uotechnology.edu.iq).

ABSTRACT: Poly(imide) (PI) hollow fiber membranes were prepared by using classical phase inversion process. Effects of different external coagulation bath temperatures (ECBT) and various bore flow rates (BFR) on the morphology and separation performance of the membranes were studied. Cross-section, inner and outer structures were characterized by using scanning electron microscope and atomic force microscopy (AFM). Mean pore size, pore size distribution, and mean roughness of the PI hollow fibers surfaces were estimated by AFM. It was found that the hollow fibers morphology composed of sponge-like and finger-like structures with different ECBT and BFR. A circular shape of the nodules with different sizes was observed in the outer surface of the PI hollow fibers. Mean pore size of the outer surface increases with increasing ECBT and BFR. The important result observed in this study is that the ECBT clearly has the largest effect on hollow fiber PI membrane roughness compared with the BFR. Pure water permeability of the PI hollow fibers was improved with increase of ECBT and BFR. The solute rejection (R%) was reduced when the ECBT and BFR was increased. © 2014 Wiley Periodicals, Inc. J. Appl. Polym. Sci. **2014**, *131*, 40428.

KEYWORDS: membranes; morphology; polyimides; separation performance; characterization

Received 19 November 2013; accepted 13 January 2014
DOI: 10.1002/app.40428

INTRODUCTION

Research and development of membrane technology deals mainly with suitable membrane materials and their fabrication in order to enhance the performance of the membranes for separation, purification, and concentration processes.[1]

It is well known that the fabrication of hollow fiber membranes affected by several factors during the formation process, for example, the viscosity of the polymer solution, the spinneret design, take-up velocity, composition and flow rate of the bore liquid, air-gap length, dope extrusion rate, and internal and external coagulation bath temperatures (ECBT), etc.[2]

In recent years, some researchers focused their studies on the effect of the ECBT on the structure and performance of the membranes prepared from polyethersulfone (PES), ethylene/vinyl acetate copolymer, cellulose acetate (CA), and poly(vinylidenefluoride) (PVDF). For example, Shina et al.[3] reported that the change of the ECBT had a pronounced effect on the pore size and the porosity of the PES membrane. Whereas, Amirilargani et al.[4] reported that increasing ECBT results in macrovoid formation in the PES membrane structure and increases the membrane permeability and decreases the protein rejection.

The effects of the coagulation bath temperature on the morphology of ethylene/vinyl acetate copolymer membranes were also investigated by Sadeghi et al.[5] It was observed that the porosity of the membranes decreased with an increase in the temperature of the coagulation bath. Moreover, Li et al.[6] prepared PES membranes by using immersion precipitation combined with the vapor induced phase separation method. It was found that ECBT had large effect on the precipitation rate; high temperature on coagulation bath mainly increases the exchange rate of solvent and non-solvent. Porous skin layer with higher flux could be obtained at a high coagulation bath temperature.

Cellulose acetate butyrate (CAB) hollow fiber membrane was prepared by using both thermally induced phase separation and non-solvent induced phase separation methods.[7] It was revealed from atomic force microscopic (AFM) images that both the nodular structure size and the roughness of the membrane outer surface were affected by the coagulation bath temperature.

Asymmetric CA membranes were synthesized by the phase-inversion method using polyvinylpyrrolidone (PVP) and polyethylene glycol (PEG) as additives.[8,9] They found that by using PVP as additive and increasing ECBT from 0°C to 25°C resulted in increasing pure water flux (PWF). Further increase of CBT

from 25°C to 50°C results in reduction of PWF.[8] While using PEG as additive and increasing the CBT resulted in increased PWP and insulin/HAS transmission.[9]

Asymmetric CA membranes were prepared from polymeric blend of CA/PEG/N-methyl-2-pyrrolidone (NMP) system via phase inversion induced by immersion precipitation in water coagulation bath.[10] It was reported that using cold coagulation bath results in reduction of membranes porosity and permeability.

The poly(vinylidenefluoride)-graft-poly(N-isopropylacrylamide) (PVDF-*g*-PNIPAAm) membranes prepared by Guo et al.[11] at different temperatures formed finger-like pores and showed higher water flux and porosity than PVDF membranes. In particular, a membrane prepared at 30°C had the largest finger-like pores and greatest porosity. The water flux of a membrane prepared in a 25°C coagulation bath showed a sharp increase when the temperature was increased to about 30°C.

Amirilargani et al.[12] found that increasing ECBT accelerates diffusional exchange rate of solvent and non-solvent fluids and formed macrovoids in the PES ultrafiltration (UF) membrane structure. Also, the effect of coagulation bath temperature on the morphology of wet-spun polyacrylonitrile fibers was investigated by Sobhanipour et al.[13] Fibers were fabricated at two coagulation bath temperatures of 5°C and 60°C. The shape of nascent fibers cross-section transforms from bean to circular and pore size increases with coagulation temperature. The average pore size and pore volume of the fibers increase with coagulation temperature. Mousavi et al.[14] found that addition of the surfactant (polyoxyethylene sorbitan monolaurate) in the PSF casting solution along with increasing the ECBT incites the formation of the bigger pores on the top surface and results in the formation of membranes with higher thickness and more porous structure in the sub-layer. Madaeni et al.[15] found that the effect of the coagulation bath temperature and evaporation time on membrane morphology of PVDF microfiltration membrane was correlated to the temperature difference between the coagulation bath and the polymer solution. Regarding the effect of ECBT on the performance of the composite membranes, Abedini et al.[16] observed that high ECBT with high concentration of TiO_2 in the polymer solution resulted in increasing the thickness, porosity, and pure water flux of CA membrane.

From the literature mentioned above it can be inferred that the different bath temperature have different effect on the morphology and separation performance of various types of membranes and there is no general trend of the effects of the bath temperature on the different types of membranes.

Regarding the flow rate of the internal coagulant it was found from the literature that few researchers studied extensively the effect of flow rate of the internal coagulant on the characteristics of the hollow fiber membranes.[17–21] Chung et al.[17] suggests that, in order to yield a high permeance as spun PES membrane with skin layer of approximately 500 Å, there might not exist a critical solvent molar volume when preparing the dope solvent mixture. The key to fabricate ultrathin PES skin-layer hollow fiber membranes with a skin layer of approximately 500 Å was in controlling both the chemistry and bore fluid flow rate of the internal coagulant. Aptel et al.[18] studied the effect of the flow rate of the internal coagulant on the polysulfone ultrafiltration characteristics. Their results showed, as the water flux inside the nascent fiber increased from 4×10^{-2} to 6×10^{-2} (cm^3/sec) the hydraulic permeability increases. Whereas, rejection for PVP ($M_w = 10{,}000$ Da) decreased from 80% to 40%. The effect of spinning conditions such as the flow rate of the internal coagulant and the composition, flow rate and temperature of the polymer solution on the geometry and performance of PES hollow fibers was studied by Mok et al.[19] It was reported that the ratio of the outer radius to inner radius decreases with increasing of the flow rate of the internal coagulant. The effects of internal coagulant flow rate (5 or 7.5 mL/min) on the characteristics of PES hollow fiber membranes produced by the solution spinning technique were also studied by Miao et al.[20] It was found that an increase in internal coagulant flow rate at a constant air gap distance tended to increase OD and ID and to decrease wall thickness for the resulting fibers. The UF separation (%) of PEG solutes and the membrane permeated product rates decreased with an increase in internal coagulant flow rate. Qin and Chung[21] reported that when bore fluid flow rate decreased, the inner diameter of spun PES hollow fiber decreased while the outer diameter remained almost the same. Moreover, when bore fluid flow rate decreased the mass transfer reduced at the inner surface but relatively increased at the outer surface, resulting in an increase in the length of finger-like macrovoids.

The main goal of this study was to investigate the influence of ECBT and flow rate of the bore fluid during the PI membrane preparation due to their significant effects on the structural morphologies and performance of PI hollow fiber membranes for removal of dyes at low pressure applications. One of the objectives of this research is to study by means of AFM both the inner and outer surfaces of PI hollow fibers. Their cross-section was characterized by scanning electron microscopy (SEM) technique. Moreover, pure water flux and solute rejection tests were conducted using methylene blue as a solute.

EXPERIMENTAL WORK

Materials

The Matrimid 5218 (polyimide of 3,3′,4,4′-benzophenone tetracarboxylic dianhidride and diamino-phenylindane) (powder form) was obtained from Ciba Specialty Chemicals and Huntsman. The solvent N,N dimethyl acetamide (DMAc) was purchased from Sigma–Aldrich Chemical Co. Methylene blue (M_w: 373.9 Da) were used as a solute and obtained from HiMedia Laboratories Pvt. Ltd. Mumbai, India.

Preparation of Dope Solution and PI Hollow Fiber NF Membranes

PI is dried in an oven at 70°C to remove the moisture content. The polymer powder was added to the DMAc solvent in a glass flask (26 : 74) (wt %) and mixed by using magnetic stirrer (250 rpm at 50°C) for 2 days until the polymer solution became homogenous. The dope solution was kept in the oven for several hours in order to remove the bubbles. Then, the dope solution was loaded in the column and compressed to the spinneret by using nitrogen gas and the internal coagulant was pumped

Table I. Spinning Parameters of the PI Hollow Fiber Membranes

(PI) composition (wt %) (g)	(PI : DMAC)	(26 : 74)			
BFR (mL/min)	1.5	2	4	4	4
Air gap length (cm)	2.5				
ECBT (°C)	30	30	30	40	50
External coagulant	Tap water				
Bore fluid	Distilled water				
Spinneret dimensions (ID : OD) (mm)	0.5 : 0.9				

to the spinneret using precision gear pump (I. Technology Engineering Co., Guro-Gu, South Korea). More details may be found elsewhere.[22,23] All spinning conditions are listed in Table I.

After spinning, the prepared PI hollow fibers were kept in water bath for 24 hr to make sure that all residual DMAc removed and then the hollow fibers transferred to the 35 wt % glycerin solution container and kept for 48 hr to prevent the collapse of the structure of the hollow fibers.

Characterization of the PI Hollow Fibers Surface

SEM. SEM measurements were used to visualize cross-section characteristics of the PI hollow fiber membranes. SEM pictures were made with a TESCAN VEGA3 SB instrument (EO Elektronen-Optik-Service GmbH, Germany) with an accelerating voltage of 30 keV. Cross-sections were prepared by fracturing the membranes in liquid nitrogen.

AFM. PI hollow fiber membrane was subjected to extensive surface analysis using an AFM of Angstrom Advanced Inc. (United States), model AA3000, in contact mode with a suitable silicon tip. All information about the AFM measurements was explained in details elsewhere.[22,24]

Pure Water Permeability (PWP) and Solutes Rejection

The performance of PI hollow fiber membranes was conducted using cross-flow filtration unit as shown in Figure 1. Three hollow fiber membranes of each type were tested under 1 bar transmembrane pressure and 600 mL/min feed flow rate. PWP (kg/m^2 hr bar) and solute rejection (R%) such as methylene blue (20 ppm) were estimated respectively using the following equations:

$$\mathrm{PWP} = \frac{M}{t \times A \times \Delta P} \tag{1}$$

$$R(\%) = \left[1 - \frac{C_P}{C_f}\right] \times 100 \tag{2}$$

where M is the mass of the collected permeate (kg), t is the collected time (hr), ΔP is the trasmembrane pressure (bar), A is the effective surface area of the membrane (m^2), C_f and C_p are the solute concentrations in feed and permeate solution, respectively. The concentration of methylene blue was determined based on absorbance in a UV-spectrophotometer at a wavelength of 660 nm. A Shimadzu UV-1601 double beam spectrophotometer was used to determine the concentration of methylene blue.

RESULTS AND DISCUSSION

The inner and outer diameters and the thickness of the PI hollow fibers prepared under different bore flow rate (BFR) and ECBT are summarized in Table II. It can be noticed that the inner and outer diameters of the PI hollow fiber membranes

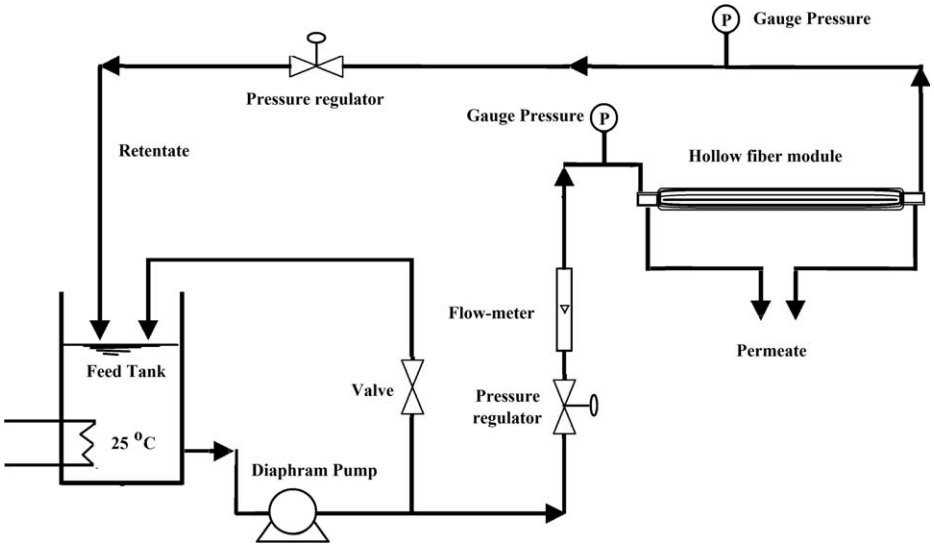

Figure 1. Schematic diagram of the cross-flow filtration unit.

Table II. Effect of BFR and ECBT on PI Hollow Fiber Membrane Dimensions

Membrane code	Temperature °C	BFR (mL/min)	D_i (μm)	D_o (μm)	Thickness (μm)	D_o/D_i
1	30	1.5	510	694.6	92.3	1.36
2	30	2	666	799.2	66.6	1.2
3	30	4	785.6	851.3	32.85	1.08
4	40	4	542.86	742.86	100	1.37
5	50	4	732.6	836.9	52.15	1.14

increases and the thickness decreases with the increase of the bore fluid flow rate (i.e., 1.5, 2, and 4 mL/min). This phenomenon is attributed to the high inner coagulant pressure in lumen side of the hollow fiber with increase of bore fluid flow rate, which causes a thin membrane thickness and large membrane diameters. Miao et al.[20] reported that an increase in BFR at a given air gap length tended to increase the inner and the outer diameters and led to decrease the thickness of the membrane wall. It can also be seen from Table II that there is no clear trend of the effect of ECBT on the dimensions of the PI hollow fiber membranes.

Figure 2 shows the SEM images of the cross-sectional area of the PI hollow fiber membranes at different bore fluid flow rates. It can be noticed that a sponge-like structure observed near the inner and outer surface of the membrane, whereas, long and thin finger-like layer observed in the middle of the cross-section and converge near the inner surface of the PI membrane prepared from 1.5 mL/min BFR, as shown in Figure 2(A). In Figure 2(B), it can be noticed that the sponge-like structure increases toward the middle of the cross-section of the membrane while the finger-like layer became short and wide with increasing of the BFR to 2 mL/min. Further increase in BFR up to 4 mL/min the cross-section of the PI membranes is changed to completely sponge-like structure with small sphere voids in the middle of the cross section as shown in the Figure 2(C). Among the key parameters controlling the hollow fiber membrane morphology is the flow rate of the bore fluid. Therefore, govern coagulant operation leads to the formation of different layers on the internal morphology of the hollow fiber membranes. However, as soon as the polymer solution gets out from the nozzle of the spinneret the solidification process of the polymer solution by the internal coagulant (water) take place. This solidification process leads to the formation of a skin layer, which served as a barrier to the further penetration of the nonsolvent (water) through the wall of the nascent fiber toward the outer surface. In this case delay solvent–nonsolvent demixing process after the skin layer occurs, resulted to the formation of sponge-like structure. With increasing the internal coagulant flow rate the skin layer formed quickly and thus further delay solvent–nonsolvent demixing process occur. This phenomenon resulted in a shift of finger-like to sphere-like structure and moved toward the middle of the fiber cross-section with more sponge density. Moreover, it can be seen from Figure 2 that the length of the sponge layer between the finger-like layer and the outer surface had not been harmed during the solidification process of the inner surface at different flow rates of the internal coagulant. This phenomenon is attributed to the remained the viscosity of the polymer solution on the outer surface unchanged during movement of the nascent fiber through the air gap distance.

Figures 2 and 3 show the SEM images of the cross-section of the PI hollow fiber membranes prepared from different ECBT (i.e., 30°C, 40°C, and 50°C). In the previous paragraph we have already explained the SEM image of the PI hollow fiber membranes prepared from 4 mL/min BFR and 30°C ECBT [see Figure 2(C)]. As can be noticed from Figure 3(A), the structure of the cross-section is sponge-like structure with voids in the shape of teardrop spread in the middle of the cross-section of the PI membrane prepared from 40°C ECBT. From Figure 3(B), it can also be noticed that the cross-section structure of the PI membrane prepared at 50°C ECBT is composed of double layers finger-like structure. It is worthy to mention here that increasing of ECBT results to change the structure of the hollow fiber from sponge structure with small finger-voids to fully finger-like structure. The speed of the liquid–liquid demixing process during the nascent hollow fiber formation affects the structural morphology of the hollow fiber membranes as reported by Kesting.[25] Instantaneous liquid–liquid demixing process results in the formation of finger-like voids in the cross-section structure of the membranes. On the contrary, delay liquid–liquid demixing process results in a sponge-like structure. In this case increasing ECBT led to an increase in the exchange rate between the water (nonsolvent) and the DMAc (solvent) in the dope solution during coagulation process therefore the structural morphology changed from sponge to finger-like structure with an increase of ECBT. In addition, Tang et al.[26] explained this phenomenon by the decreased viscosity of dope solution as ECBT increases, which enhanced the exchange rate between DMAc solvent and the water coagulant for phase inversion. These results are in good agreement with that reported in the literature.[4,10]

Three dimensions AFM images of the outer surface over an area of 1.5×1.5 μm^2 for PI hollow fiber membranes prepared from different bore fluid flow rates and external coagulation temperatures are shown in Figure 4. It can be seen that the nodular structure is formed in the outer skin of the outer surface of the PI hollow fiber membranes. The circular shape nodules with different sizes was observed to form in the outer surface of the PI hollow fiber membranes prepared from 1.5 mL/min BFR [see Figure 4(A)]. The circular shape nodules coalesce with each other and form nodules in the shape of lane with an increase of

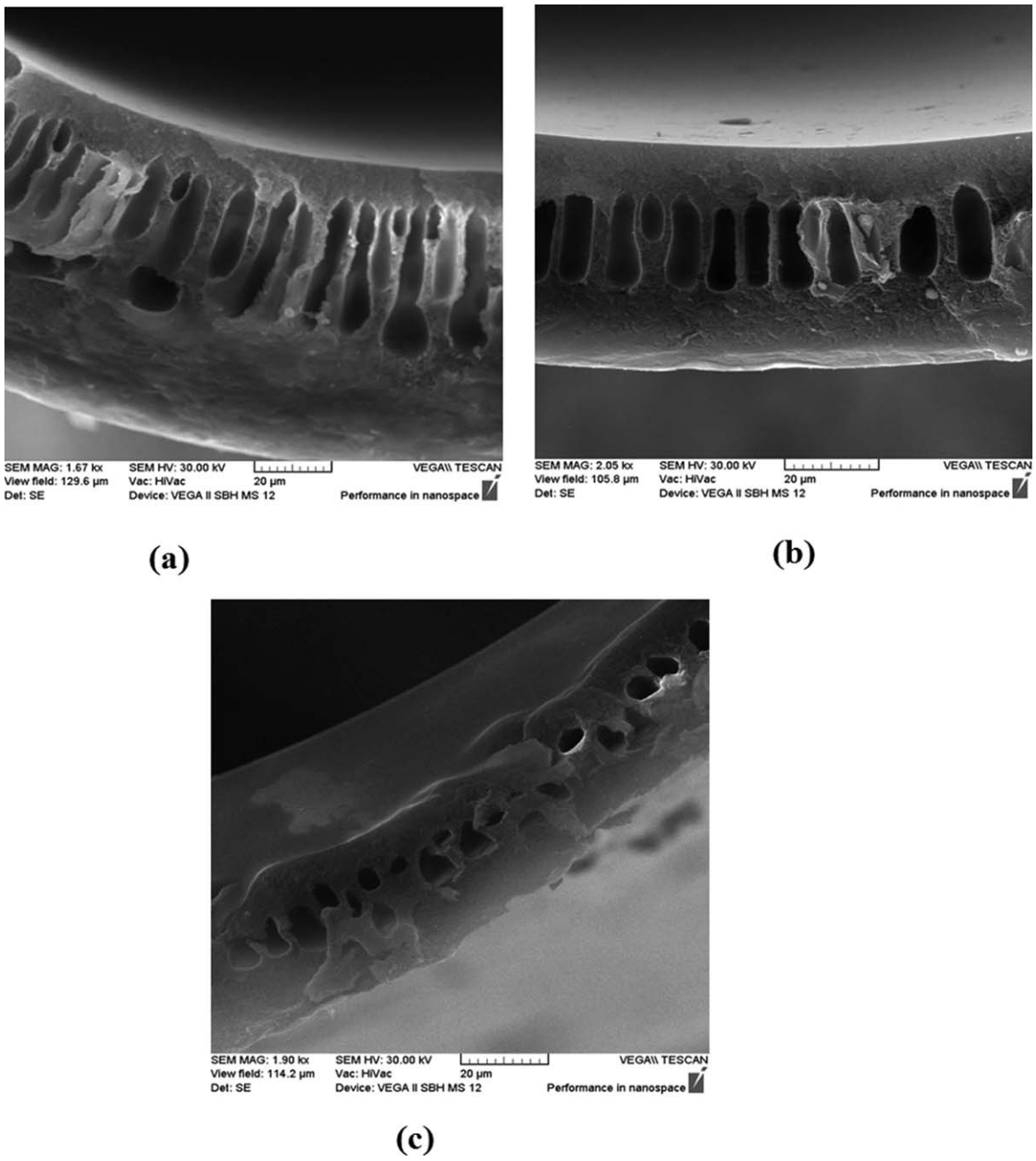

Figure 2. SEM images of the cross-sectional area of PI hollow fiber membranes prepared from different BFR at 30°C (**A**) 1.5 mL/min, (**B**) 2 mL/min, and (**C**) 4 mL/min.

BFR to 2 and 4 mL/min as shown in Figure 4(B,C). It is important to mention here that there is a strong effect of the BFR on the outer surface of the hollow fiber membranes. The possible reason for this observation is due to the stretching of the outer surface of the membrane as a result of bore fluid pressure on the membrane surface with increasing of BFR during the nascent hollow fiber membrane formation. A similar shape was found at the inner surface of the PI hollow fiber prepared from 1.5 mL/min as can be seen in Figure 5(A). Further increase in BFR results to reduce the size of the circular shape nodules with an increase of the nodules density as shown in Figure 5(B,C). Figures 4(C) and 6 show the AFM images of the PI hollow fiber membranes with the increase of ECBT from 40°C to 50°C. An increase in ECBT resulted to an increase of the circular nodule sizes due to the rapid exchange rate between hot water in external coagulation bath and DMAc solvent at the outer surface of the PI hollow fibers as shown in Figures 4(C) and 6(A,B). There are two different phase separation mechanisms that took place during the formation of the hollow fiber membrane skin: first; when a polymer solution becomes thermodynamically unstable**:** nucleation and growth (delay liquid–liquid demixing process) or spinodal decomposition (fast liquid–liquid demixing process). It is believed that these two mechanisms took place during the formation of the PI hollow fiber skin. Delay liquid–liquid demixing process also took place during the formation of the membranes prepared from PI solution resulting in inner

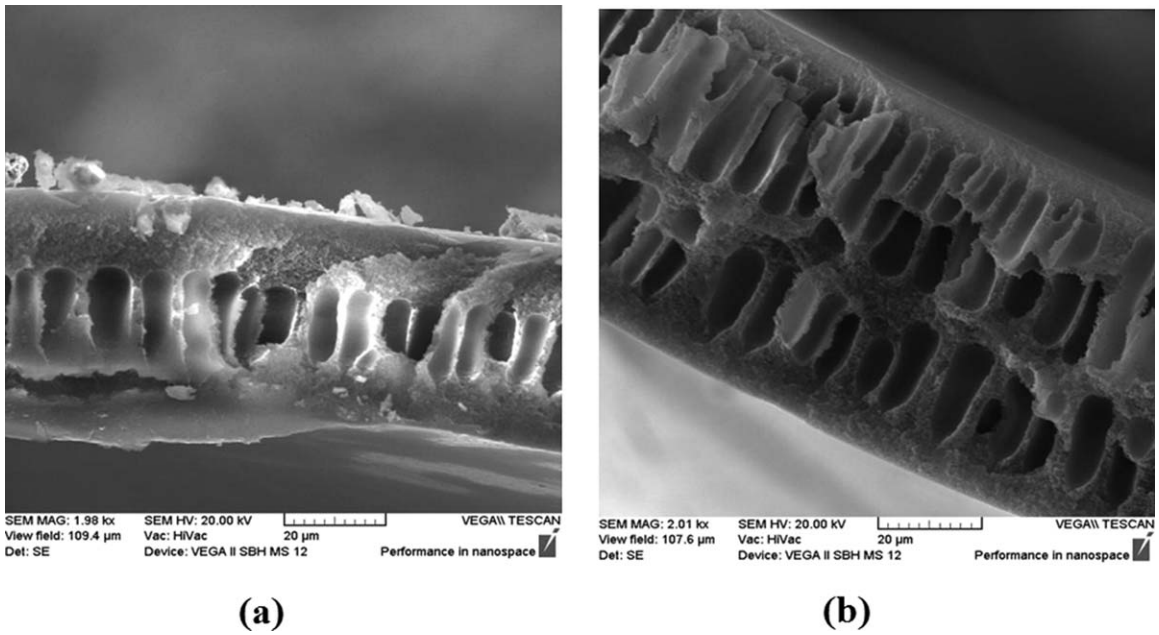

Figure 3. SEM images of the cross-sectional area of PI hollow fiber membranes at different ECBT (**A**) 40°C and (**B**) 50°C.

surfaces that are fully porous. Meanwhile, rapid liquid–liquid demixing process at the outer surface of the PI hollow fibers took place when the coagulation bath temperature was increased.

The mean pore size and the mean roughness (R_a) (the mean value of the surface relative to the center plane) is evaluated over an area of 1.5 × 1.5 µm^2 are shown in Table III. It can be seen that there is no clear trend of the effect of the BFR on the

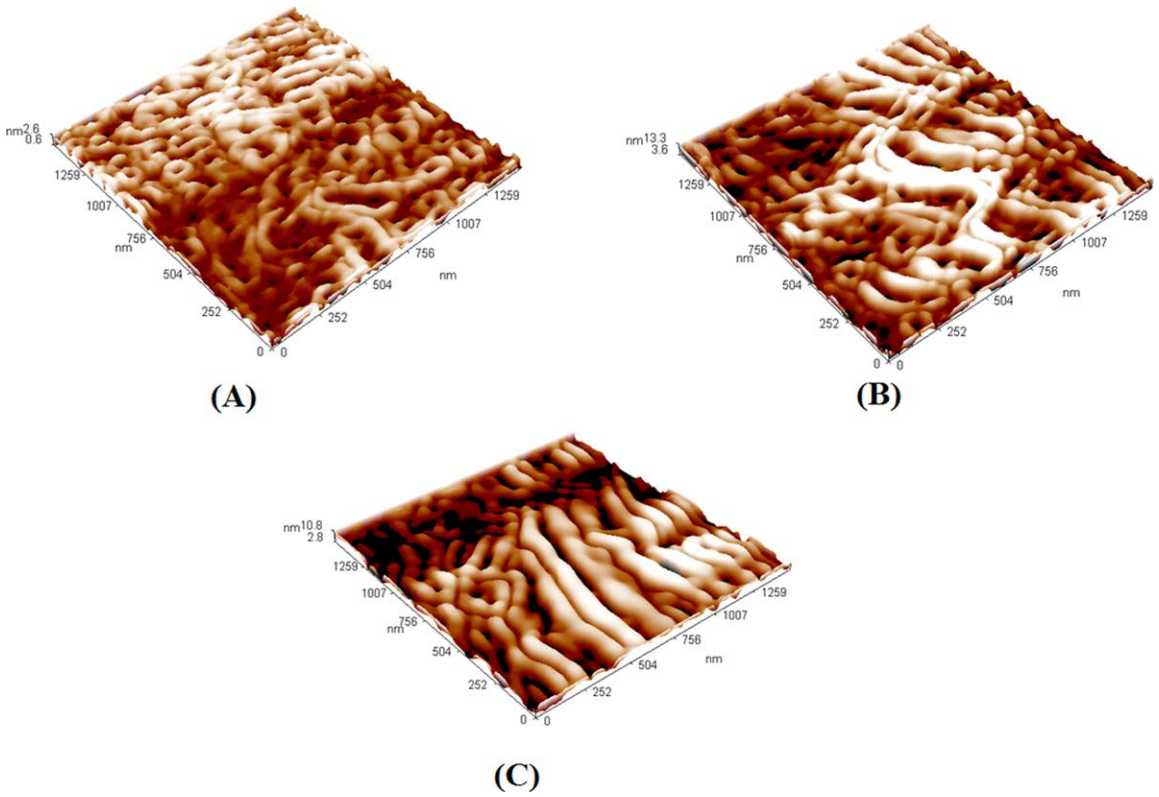

Figure 4. Three dimensions AFM images of the outer surface of PI hollow fiber membranes prepared from different BFR at 30°C ECBT: (**A**) 1.5 mL/min; (**B**) 2 mL/min; and (**C**) 4 mL/min. [Color figure can be viewed in the online issue, which is available at wileyonlinelibrary.com.]

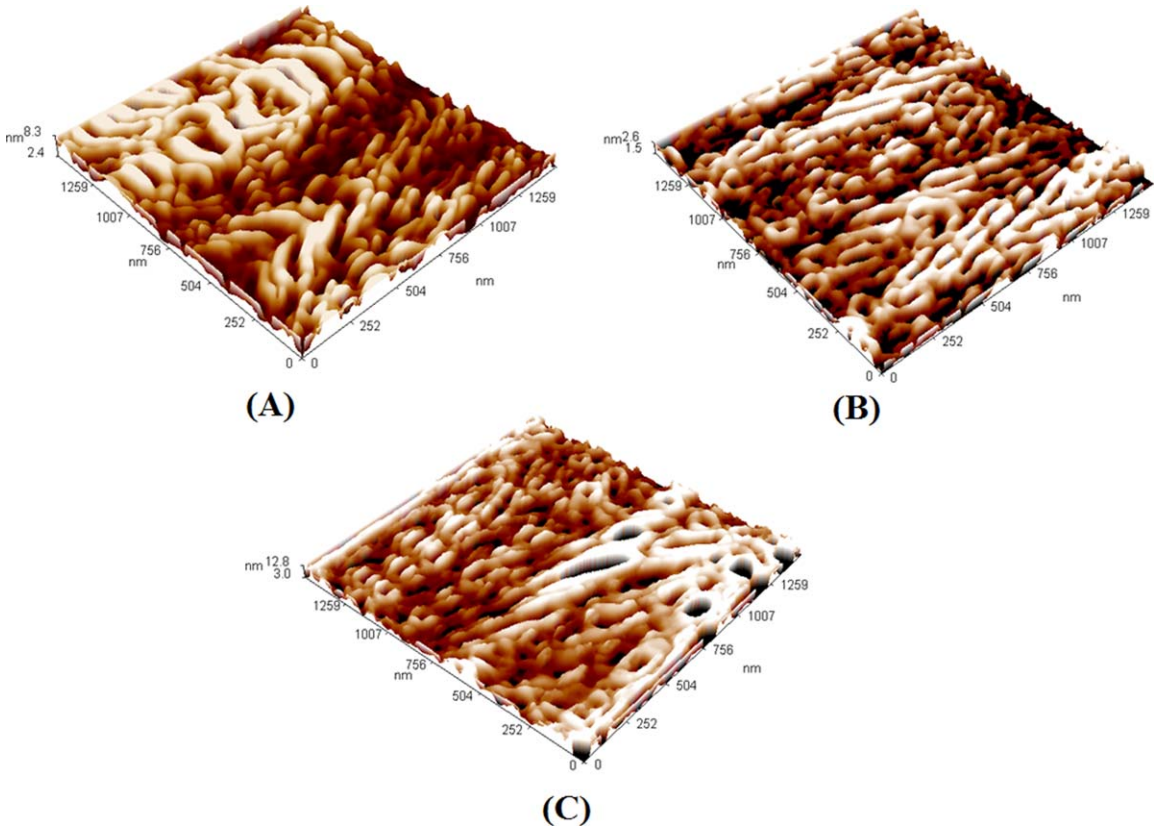

Figure 5. Three dimensions AFM images of the inner surface of PI hollow fiber membranes prepared from different BFR at 30°C ECBT: (**A**) 1.5 mL/min; (**B**) 2 mL/min; and (**C**) 4 mL/min. [Color figure can be viewed in the online issue, which is available at wileyonlinelibrary.com.]

mean pore size and mean roughness of the inner surface of the PI hollow fibers with significant effect of the ECBT on mean roughness as shown in Table III. Moreover, in Table III it can be noticed that the mean pore size increases with increasing of BFR, and there is no trend effect on the mean roughness of the outer surface of PI hollow fiber membranes. With an increase of the ECBT from 30°C to 40°C the mean pore size decreased, whereas the mean pore size increased highly with an increase of the external temperature to 50°C as shown in Table III. These phenomena are due to the different structural morphologies of the prepared PI membranes. This is because of the various liquid–liquid demixing speed between the nonsolvent and polymer solvent with an increase of ECBT. It is worth to mention here that the important result observed in this study is that the ECBT clearly has the largest effect on hollow fiber PI membrane roughness compared with the bore fluid flow rate, which is not reported yet in the literature. The exchange rate between solvent in polymer solution and water bore fluid plays a major role in

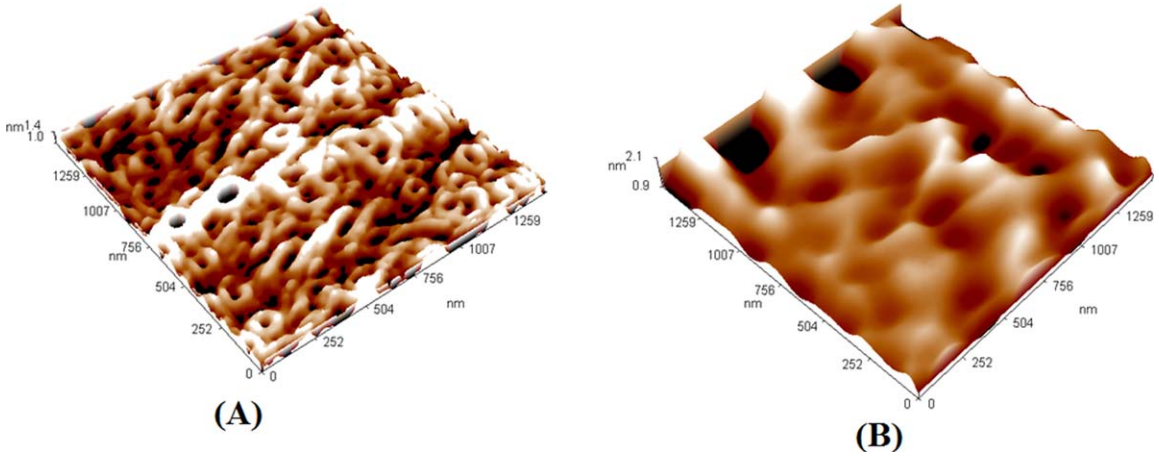

Figure 6. Three dimensions AFM images of the outer surface of PI hollow fiber membranes prepared from different ECBT: (**A**) 40°C and (**B**) 50°C. [Color figure can be viewed in the online issue, which is available at wileyonlinelibrary.com.]

Table III. Mean Pore Size and Mean Roughness of the Inner PI Hollow Fiber Membrane Surface

	Inner surface (1.5 × 1.5 μm^2)		Outer surface (1.5 × 1.5 μm^2)	
Membrane code	Mean pore size (nm)	Mean roughness R_a (nm)	Mean pore size (nm)	Mean roughness R_a (nm)
1	90.42	1.45	56.39	0.443
2	77.27	0.337	118.43	2.67
3	86.03	2.65	173.29	2.18
4	55.66	0.175	117.29	0.128
5	103.73	0.354	228.10	0.215

determining the morphology of the inner and outer surface of the membrane in addition to the membrane dimensions, as well as the size and distribution of the pores on the surface. Therefore, the ECBT has a significant effect on the roughness of PI membranes due to its effect on the inner and outer surface of the membrane as compared with the effect of BFR on the inner surface of the membrane with a minor effect on the outer surface.

From the results presented in Table III, it can be concluded that the structure of PI hollow fiber membranes can be classified as anisotropic structure, where the pores change in size from one surface of the membrane to the other.

Effects of BFR on the pore size distribution of the PI hollow fiber surfaces are shown in Figures 7 and 8. It can be noticed from Figure 7(A) that a wide pore size distribution from 65 to 215 nm is obtained for the inner surface of PI hollow fibers prepared from 1.5 mL/min BFR. With an increase of BFR to 2 and 4 mL/min the pore size distribution decreases and became narrow (i.e., 60–125 nm) in Figure 7(B,C). Narrow pore size distribution between 35 and 125 nm was observed on the outer surface of the PI hollow fibers prepared by using 1.5 mL/min BFR in Figure 8(A). Further increase of BFR to 2 mL/min the pore size distribution start to be become wider (i.e., between 80 and 250 nm) as shown in Figure 8(B). With 4 mL/min BFR the pore size distribution was between 130 and 250 nm [see Figure 8(C)].

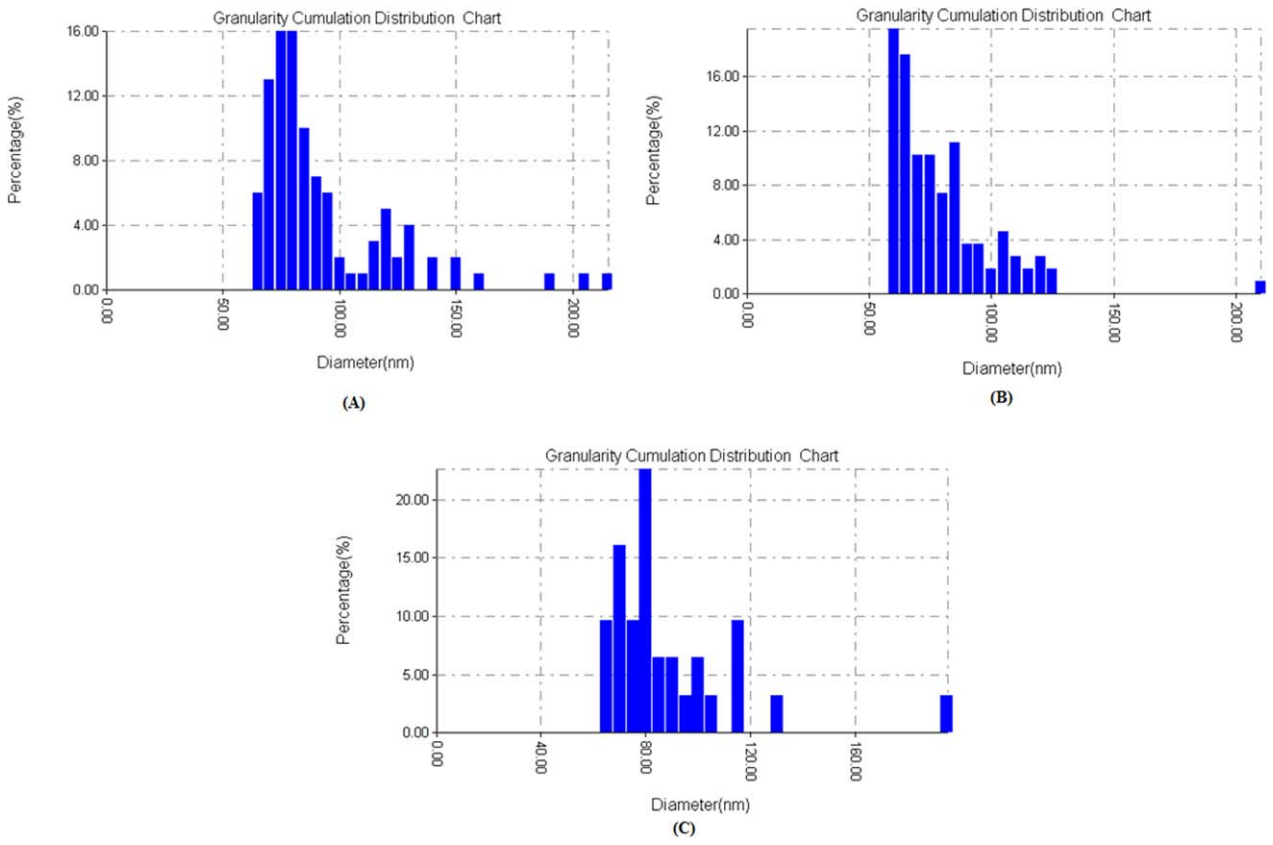

Figure 7. Pore size distribution of the inner surface at different BFR: (**A**) 1.5 mL/min; (**B**) 2 mL/min; and (**C**) 4 mL/min. [Color figure can be viewed in the online issue, which is available at wileyonlinelibrary.com.]

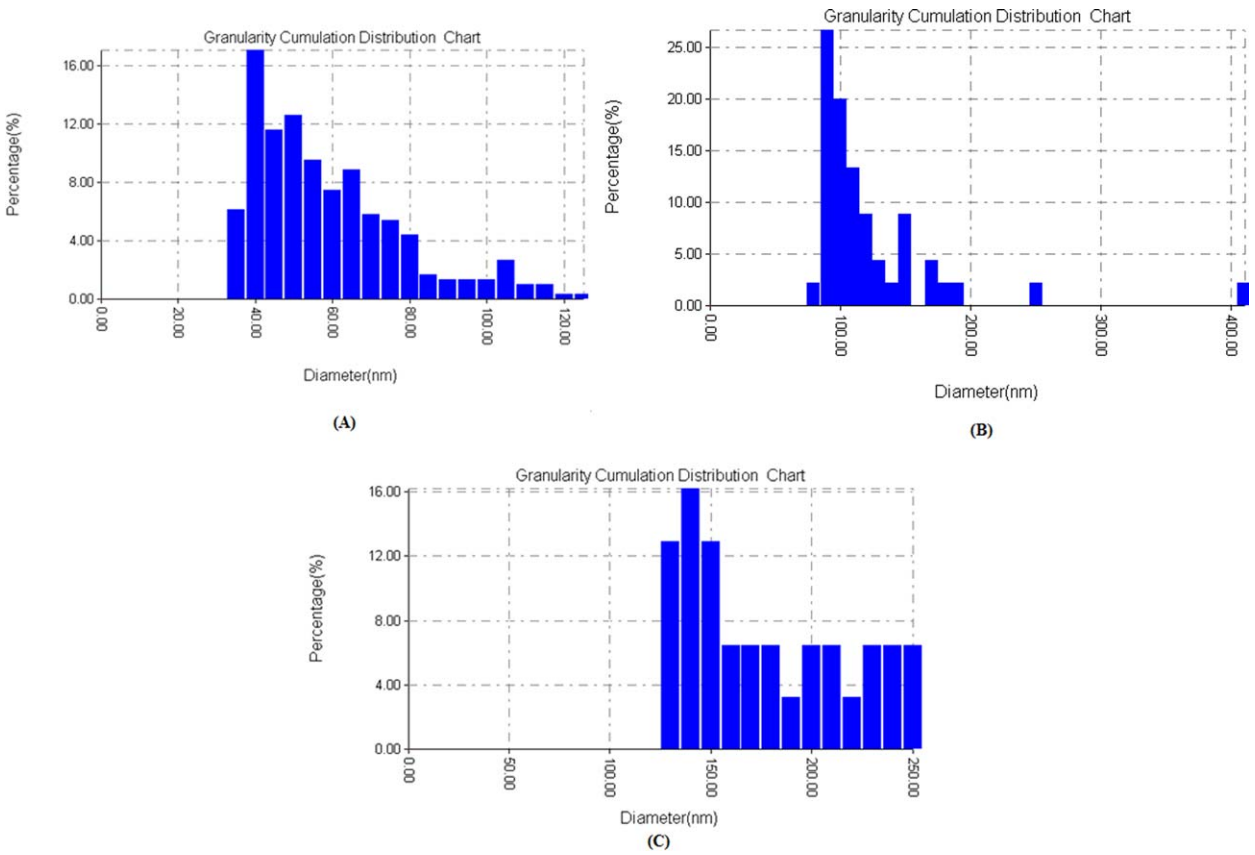

Figure 8. Pore size distribution of the outer surface at different BFR: (**A**) 1.5 mL/min, (**B**) 2 mL/min, and (**C**) 4 mL/min. [Color figure can be viewed in the online issue, which is available at wileyonlinelibrary.com.]

Effects of coagulation bath temperature on the pore size distribution of the PI hollow fiber surfaces are shown in Figures 9 and 10. It can be noticed that the pore size distribution of the inner surface of the PI hollow fibers was between 45 and 130 nm with 40°C coagulation temperature [Figure 9(A)]. On the other hand, increasing the coagulation temperature up to 50°C resulted to a wide distribution between 80 and 240 nm as shown in Figure 9(B). Regarding the outer surface it can be seen from Figure 10(A) that the pore size distribution was between 100 and 190 nm, whereas the pore size distribution was between 180 and 300 nm with an increase of the coagulation temperature to 50°C as shown in Figure 10(B).

In solute transport experimental test shown in Figure 1, the feed solution was pumped through the lumen side of the hollow fiber membranes and the permeate solution was collected from

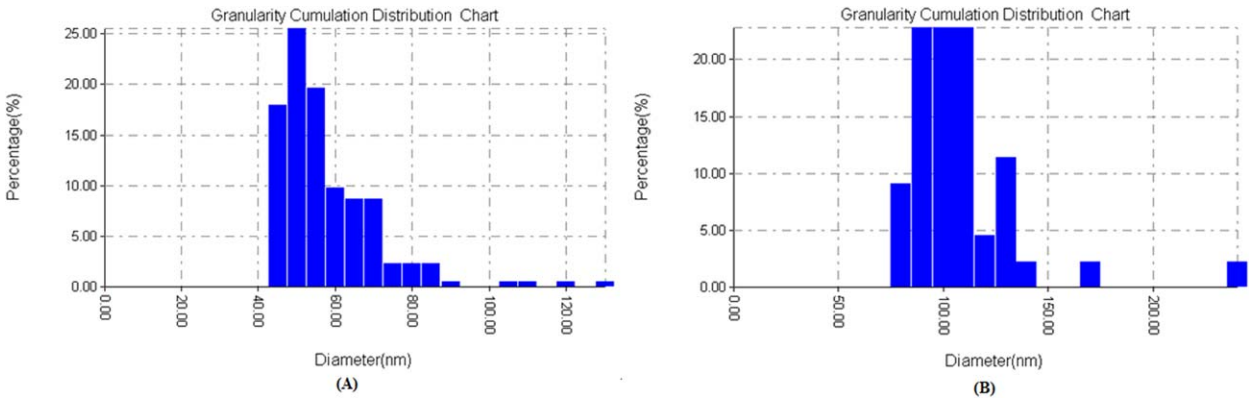

Figure 9. Pore size distribution of the inner surface at different ECBT temperatures (**A**) 40°C and (**B**) 50°C. [Color figure can be viewed in the online issue, which is available at wileyonlinelibrary.com.]

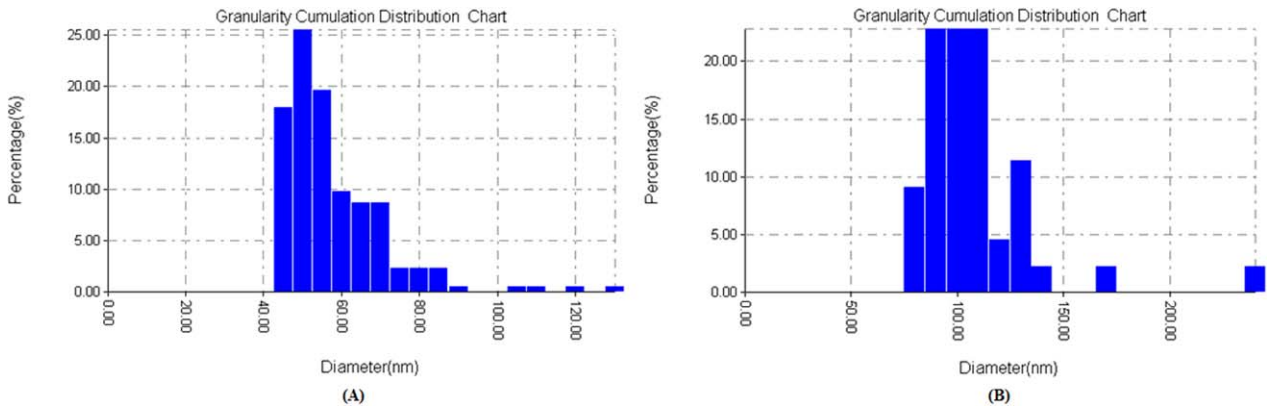

Figure 10. Pore size distribution of the outer surface at different ECBT temperatures (**A**) 40°C and (**B**) 50°C. [Color figure can be viewed in the online issue, which is available at wileyonlinelibrary.com.]

the shell side of the membrane module. This indicates that the inner-edge of the surface through the cross-section of the PI hollow fiber membranes that controls the pure water permeation flux and solute rejection of the PI hollow fiber membrane.

Table IV shows the effects of bore fluid flow rates and temperature of the external coagulation bath on the performance of the PI hollow fiber membranes. It can be noticed that the pure water flux increases whereas the solute rejection decreases when the bore fluid flow rate was increased from 1.5 to 4 mL/min. This result in principle may be due to the decrease in wall thickness of the PI hollow fibers with increase in BFR as shown in Table II and also due to the pore density of the PI hollow fibers (see Figure 4). Moreover, in Table IV it can be seen that the pure water permeation flux increases and solute rejection decreases with increase of the ECBT (i.e., 30°C and 40°C). Further increase in ECBT results in decrease of the pure water permeation flux and increase of solutes rejection. This is due to the change in the structural morphology from sponge-like structure to finger-like structure and also due to the difference in pore density of the PI hollow fibers as discussed in detail above.[23]

In fact, in this method PI hollow-fiber membranes with a high PWP could be prepared, whereas the MB rejection of PI hollow-fiber membranes was approximately in the range of 91%–96%. Therefore, it can be concluded that these types of hollow fibers are suitable for removal of dyes from industrial wastewater.

CONCLUSIONS

PI hollow fiber membranes were prepared by using classical phase inversion process. From the results of the present study it can be concluded and recommended that:

1. The inner and outer diameters of the PI hollow fiber membranes increase with the increase in the bore fluid flow rate, while the thickness of the membrane decreases with an increase in the fluid flow rates. This phenomenon is attributed to the high inner coagulant pressure with the increase of the bore fluid flow rate. Moreover, there is no clear trend of the effect of ECBT on the dimensions of the PI hollow fiber membranes.
2. Cross-section structure of PI hollow fibers membrane were changed from sponge-like structure observed near the inner and outer surface of the membrane and long and thin finger-like layer observed in the middle of the cross-section to completely sponge-like structure with small sphere voids in the middle of the cross section with increasing of the bore fluid flow rate.
3. The circular shape of the nodules with different sizes was observed in the outer surface of the hollow fibers prepared from 1.5 mL/min BFR. The circular shape nodules coalesce

Table IV. Effect of BFR and ECBT on the Performance of PI Hollow Fiber Membranes

Membrane code	ECBT (°C)	BFR (mL/min)	Pure water flux (kg/m^2 hr bar)	MB[a] rejection (R%)
1	30	1.5	55	96
2	30	2	59.8	94
3	30	4	60	94
4	40	4	137	91
5	50	4	64.7	92.5

[a] Methylene blue.

with each other and formed nodules in the shape of lane with an increase of the BFR to 2 and 4 mL/min.

4. PWP of the PI hollow fibers were enhanced with increase of ECBT and BFR and highly PWP was observed using 40°C as ECBT. While the solutes rejection (R%) was reduced when the ECBT and BFR increased.

ACKNOWLEDGMENTS

Associate Prof. Dr. Qusay F. Alsalhy gratefully thank the Nanotechnology and Advanced Materials Research Center at the University of Technology, Baghdad, Iraq and Assistant lecturer Ketam Salim for the Scanning Electron Microscope (SEM) analyses.

REFERENCES

1. Seader, J. D.; Henley E. J. Separation Process Principles; John Wiley & Sons, Inc.: NJ, **1998**.
2. Xu, Z.-L.; Qusay Alsalhy, Q. *J. Membr. Sci* **2004**, *233*, 101.
3. Shina, S.-J.; Kimb, J.-P.; Kimb, H.-J.; Jeonc, J.-H.; Min, B.-R. *Desalination* **2005**, *186*, 1.
4. Amirilargani, M.; Saljoughi, E.; Mohammadi, T.; Moghbeli, M. R. *Polym. Eng. Sci.* **2010**, *50*, 885.
5. Sadeghi, M.; Mousavi, S. A.; Motamed Hashemi, M. Y.; Pourafshari Chenar, M.; Roosta Azad, R. *J. Appl. Polym. Sci.* **2007**, *105*, 2683.
6. Li, J.-F.; Xu, Z.-L.; Yang, H. *Polym. Adv. Technol.* **2008**, *19*, 251.
7. Fu, X. Y.; Sotani, T.; Matsuyama, H. *Desalination* **2008**, *233*, 10.
8. Saljoughi, E.; Mohammadi, T. *Desalination* **2009**, *249*, 850.
9. Saljoughi, E.; Amirilargani, M.; Mohammadi, T. *J. Appl. Polym. Sci.* **2010**, *116*, 2251.
10. Saljoughi, E.; Amirilargani, M.; Mohammadi, T. *Desalination* **2010**, *262*, 72.
11. Guo, Y.; Feng, X.; Chen, L.; Zhao, Y.; Bai, J. *J. Appl. Polym. Sci.* **2010**, *116*, 1005.
12. Amirilargani, M.; Sadrzadeh, M.; Mohammadi, T. *J. Polym. Res.* **2010**, *17*, 363.
13. Sobhanipour, P.; Cheraghi, R.; Volinsky, A. A. *Thermochim. Acta* **2011**, *518*, 101.
14. Mousavi, S. M.; Saljoughi, E.; Ghasemipour, Z.; Hosseini, S. A. *Polym. Eng. Sci.* **2012**, *52*, 2196.
15. Madaeni, S. S.; Pourghorbani, R.; Vatanpour, V. *Adv. Polym. Technol.* **2012**, *31*, 29.
16. Abedini, R.; Mousavi, S. A.; Aminzadeh, R. *Chem. Indus. Chem. Eng. Q.* **2012**, *18*, 385.
17. Chung, T. S.; Teoh, S. K.; Hu, X. *J. Membr. Sci.* **1977**, *133*, 161.
18. Aptel, P.; Abidine, N.; Ivaldi, F.; Lafaille, J. P. *J. Membr. Sci.* **1985**, *22*, 199.
19. Mok, S.; Worsfold, D. J.; Fouda, A. E.; Matsuura, T.; Wang, S.; Chan, K. *J. Membr. Sci.* **1995**, *100*, 183.
20. Miao, X.; Sourirajan, S.; Zhang, H.; Lau, W. W. Y. *Sep. Sci. Technol.* **1996**, *31*, 141.
21. Qin, J.-J.; Chung, T.-S. *J. Memb. Sci.* **2004**, *229*, 1.
22. Alsalhy, Q. F.; Rashid, K. T.; Ibrahim, S. S.; Ghanim, A. H.; Van der Bruggen, B.; Luis, P.; Zablouk, M. *J. Appl. Polym. Sci.* **2013**, *129*, 3304.
23. Alsalhy, Q.; Algebory, S.; Alwan, G. M.; Simone, S.; Figoli, A.; Drioli, E. *Sep. Sci. Technol.* **2011**, *46*, 2199.
24. Alsalhy, Q. F.; Ali, J. M.; Abbas, A. A.; Rashed, A.; Van der Bruggen, B.; Balta, S. *Desalin. Water Treat.* **2013**, *51*, 6070.
25. Kesting, R. E. Synthetic Polymeric Membranes, 2nd ed.; Wiley: New York, **1985**.
26. Tang, Y.; Li, N.; Liu, A.; Ding, S.; Yi, C.; Liu, H. *Desalination* **2012**, *287*, 326.